Flexible Low-Temperature RF Plasma Source for Biomedical Applications

Rosendo Peña-Eguiluz, *Member, IEEE*, Antonio Mercado-Cabrera, Alma N. Hernández-Arias, Benjamín G. Rodríguez-Méndez, Régulo López-Callejas, Raúl Valencia-Alvarado, and Bethsabet Jaramillo-Sierra

***Abstract*—A flexible low-temperature plasma (LTP) source device was developed utilizing a radiofrequency (RF) generator coupled to a coaxial cable through a homemade L-shape matching network and a supple plastic hose that conveys a gas flow and shields the coaxial cable up to the reactor's nozzle. The impedance matching network provides an electric power transfer of minimum of 94.11% operating under normal conditions. The LTP device arrangement is described, and later characterized via optical emission spectroscopy and electric power consumption. This procedure is essential to determine the adequate application of the generated plasma over heat-sensitive materials, primarily organic matter, to provide adequate information about its physicochemical activity. The produced LTP interacts with surrounding air particles, generating reactive oxygen and nitrogen species (RONS) that exhibit bactericidal and antiseptic properties due to their strong biochemical reactivity. The electromagnetic irradiation, ultraviolet (UV) emission, and thermal surface effect produced under normal working conditions of the LTP source device are safe to apply to heat-sensitive matter. The device's inactivation property was validated through qualitative deactivation trials of *Escherichia coli* and *Enterococcus faecalis* and quantitative deactivation trials of *Escherichia coli*. The device inactivated 99.996% of *E. coli* at a concentration of 3.6×10^6 colony forming units per mL (CFU/mL) in 180 s at 16 W, this result corresponds to a 4.43-$\log_{10}$ reduction in *E. coli* viability.**

Link to graphical and video abstracts, and to code: https://latamt.ieeer9.org/index.php/transactions/article/view/9847

***Index Terms*— engineering in medicine and biology, low-temperature plasmas, optical emission spectroscopy, plasma applications, plasma devices.**

The associate editor coordinating the review of this manuscript and approving it for publication was Guadalupe Dorantes-Mendez (*Corresponding author: Rosendo Peña-Eguiluz*).

Rosendo Peña-Eguiluz, A. Mercado-Cabrera, B. G. Rodríguez-Méndez, R. López-Callejas, and R. Valencia-Alvarado are with the Instituto Nacional de Investigaciones Nucleares, Ocoyoacac, Estado de México, México (e-mails: rosendo.eguiluz@inin.gob.mx, antonio.mercado@inin.gob.mx, benjamin.rodriguez@inin.gob.mx, regulo.lopez@inin.gob.mx, and raul.valencia@ inin.gob.mx).

A. N. Hernández-Arias is with Universidad Tecnológica del Valle de Toluca, Lerma, Estado de México, México (e-mail: alma.arias@utvtol.edu.mx).

B. Jaramillo-Sierra is with Tecnológico Nacional de México, Tecnológico de Estudios Superiores de Tianguistenco, Santiago Tianguistenco, Estado de México, México (e-mail: bethsabet.jaramillo@test.edu.mx).

Color versions of one or more of the figures in this article are available online at http://ieeexplore.ieee.org

I. Introduction

LOW-TEMPERATURE plasma (LTP) physics research and technology development for biomedical applications is a reality nowadays. This fact results from the outstanding efforts of many worldwide who are involved in this subject. LTP can be produced by specially designed generators constituted by an electric discharges reactor associated to an electric power supply. LTP is a non-equilibrium electric discharge where the temperature of the electrons is much higher than the temperature of the heavy species or the gas. This kind of plasma is weakly ionized wherein free electrons interact with air molecules through collisions, producing several chemical reactions that generate excitation and ionization of atomic and molecular species. Some are identified as reactive oxygen and nitrogen species (RONS) like $O^{\bullet}$, OH, NO, NOγ, H_2O_2. These species can be identified by detecting the characteristic wavelength of an emitted photon during an electron's de-excitation process.

A watershed research associated with LTP applied to biomedical engineering and medicine was done with the fine surface treatment of biomaterials by the plasma needle [1]. Since then, it has been proved by several experiments that LTP deactivates numerous strains of bacteria or bacterial spores [2]-[6], denoting more than one inactivation mechanism attributed to the excitation of cells' biological molecules. Starting with the produced ultraviolet (UV) radiation, then via long-term reactions established with RONS [5]-[8]. Hence the microorganism's inactivation capability of LTP provides bactericidal effect for decontamination on materials' surfaces [4], [9]. Moreover, as LTP can interact with mammalian cells and tissues in a non-destructive behavior [10]-[12], it increases fibroblast availability and mobility [13]; accelerates healing of wounds practiced *in vivo* with mice [14]; promotes effective re-epithelialization and angiogenesis at the wound site [15]; improves collagen availability, cell proliferation, microcirculation [16], induces cell detachment and apoptosis of melanoma cells [17]-[19] with higher lethality than lymphocytes and fibroblasts [20]. These LTP's capabilities, in addition to its antisepsis capacity [21] provide beneficial healing acceleration, in contrast to conventional treatments in several clinical cases such as: burn injuries [22], [23] acute neck radiodermatitis [24], pressure ulcers [15], [25] wounds in lower extremities [26], diabetic foot [27], [28], postsurgical wound healing of a patient suffering human immunodeficiency virus [29], biopsy of the mobile oral mucosa [30], dental cavity recurrent aphthous stomatitis [31].

Studies about melanoma deactivation and antitumor potential of the LTP have been carried out as well [20], [32]-[35].

The technological development of several categories of LTP generators has supported all the cited trials above. They are classified in function of the plasma application mode, whether as: direct exposition (where plasma is projected over the target) [1], [4], [7], [8], [11], [12], [14], [15], [19] or indirect/remote exposition (where the produced plasma is forced to be in contact with the target by air convection) [2], [9], [11]. Another important variance is the nature of the electric power supply that could be dc pulsed [11], ac line frequency [25], ac very low to low frequency [2], [4], [8], [9], [15] radiofrequency (RF) [1], [12], [14], [19] microwave [7], *inter alia*. LTP generator should be characterized mainly when it is intended to be used for medical and biomedical applications [36]-[39], because a precisely knowledge of LTP properties; like the function of the supplied gas, nature of the electric source, applied electric power magnitude, exposition time and distance to the biologic matter to be treated, is crucial.

Currently, there are several flexible plasma sources, such as the one proposed in Liu *et al*., [40], where a microwave plasma source is generated on a microstrip line array where argon flowing at 5.0 LPM is projected through a flexible plastic hose. This generator requires extensive assembly that is neither portable nor feasible to implement by hand, and there is no evidence of active particle generation. A flexible DBD plasma source of 12 cm in length supplied with helium at 6.0 to 8.0 LPM, depending on the operation mode (*brush* or *comb*), with an AC voltage of 7.5 kV peak to peak at 15 kHz is shown in [41]. The device has low power consumption and provides optical emission spectroscopy (OES) spectra denoting no evidence of NOγ, which are crucial for biomedical applications. An endoscopic DBD plasma jet electric excited by an AC power source delivering an electric power from 10 W to 80 W, supplying at 18 kHz, 4.5 kV to 8.8 kV and 2 to 15 mA to a human box model is described in [42]; the plasma is generated in helium at no specified flow rate along a PTFE tube and due to the internal configuration fluorine is produced, which is known to be highly reactive, furthermore exposure to the plasma requires an electric current to flow through the target. The work of do Nascimento *et al*., [43] consists of a flexible atmospheric pressure plasma jet produced in helium flowing at 2.0 LPM by a commercial pulsed AC power source providing voltage ranging from 15 kV to 30 kV peak to peak and RMS current form 1.59 mA to 5.52 mA and a patient leakage current simulated with an RC electric circuit resulting in 33.17 μA to 63.89 μA; as in the previous case when the plasma is applied to the target electric current must flow to close the electric circuit.

In this document, the flexible NTP source is powered by a fixed RF frequency standardized for biomedical applications. The LTP generated in helium flowing at only 1.0 LPM is situated at the tip of the nozzle, avoiding interaction with any of its constituent materials and is electrically isolated from the target to be directly exposed to the plasma. This device is proposed as a viable medical device that could be integrated in endoscopy and laparoscopy tools, for instance, it could be applied as a wound healing therapy after esophageal, gastric or cervical biopsy, also to treat gastric ulcers and low-grade cervical injuries; in all cases the main goal is restoring the integrity of the compromised tissue. The implemented frame of the LTP generator; the characterization of the produced plasma using OES technique, UV emission detection, thermal and electric measurements in function of the supplied RF power; and the microbiological inactivation property is proven in a qualitative method with some experiments of bacteria inactivation for both broad categories gram-positive and gram-negative are described in this document.

II. Description

The proposed LTP device is depicted in Fig. 1. It is comprised of a 13.56 MHz RF generator model ACG-3B (ENI Technology Inc., Rochester, U.S.) coupled to a flexible LTP source through a homemade low-pass L-shaped matching network. LTP source has two inlets that meet on a 4.8 mm plastic Y-hose connector, allowing the transmission of RF signals by a 9174 RG 174/U coaxial cable and the gas supply into a 3/8" plastic hose and an outlet incorporating an RA.00.250 (LEMO, Ecublens, Switzerland) connected to a thin copper wire functioning as an energized electrode. This design is 195 cm long, has a capacitance (C_C) of 195 pF, an impedance of 8.14 kΩ and a resistance (R_C) of 18 Ω. Measurement of the electric parameters was performed with a 4263B LCR meter (Agilent, Santa Clara, U.S.) working with an internal frequency test of 100 kHz.

III. Methodology

An impedance matching network becomes indispensable to transfer the maximum power from the RF generator to the discharge reactor. Usually, a PI class network is associated with commercial generators; in the present case, due to the relatively high capacitance value of the RF cable (195 pF), it has been considered the output capacitor C_C of the PI class network. This capacitance is associated in parallel with the cable resistance R_C. Consequently, the circuit to be implemented is an L-shaped class network with an input capacitor C and a serial inductor L. Thus, the admittance $Y_L = G+jB$ connected to the RF generator is determined using its conductance G and susceptance B as follows:

$$G = R_C[(1-\omega^2 LC_C)^2 + (\omega L/R_C)^2]^{-1} \quad (1)$$

$$B = \omega C + \frac{\omega C_C(1-\omega^2 LC_C)-(\omega L/{R_C}^2)}{(1-\omega^2 LC_C)^2+(\omega L/R_C)^2} \quad (2)$$

where j is the imaginary unit, $\omega=2\pi f$ is the angular frequency and f = 13.56 MHz. For an adequate impedance matching $G=1/R_S$ and $B=0$, resulting that,

$$C_C = \left[1 + \sqrt[2]{R_S/R_C - (\omega L/R_C)^2}\right]/\omega^2 L \quad (3)$$

$$C = \frac{L/{R_C}^2 - C_C(1-\omega^2 LC_C)}{(1-\omega^2 LC_C)^2+(\omega L/R_C)^2} \quad (4)$$

The electric parameters of the matching network can be calculated from the last two expressions or via a circuit model simulation. The resulting matching circuit has an input capacitance set up by a fixed high voltage (HV) capacitor of 400 pF associated in parallel with an HV multiple parallel plate variable capacitor of 240 pF, both of which are serially linked to the output terminal via an inductor of 1.32 μH. This matching network allows the transfer of RF power from the

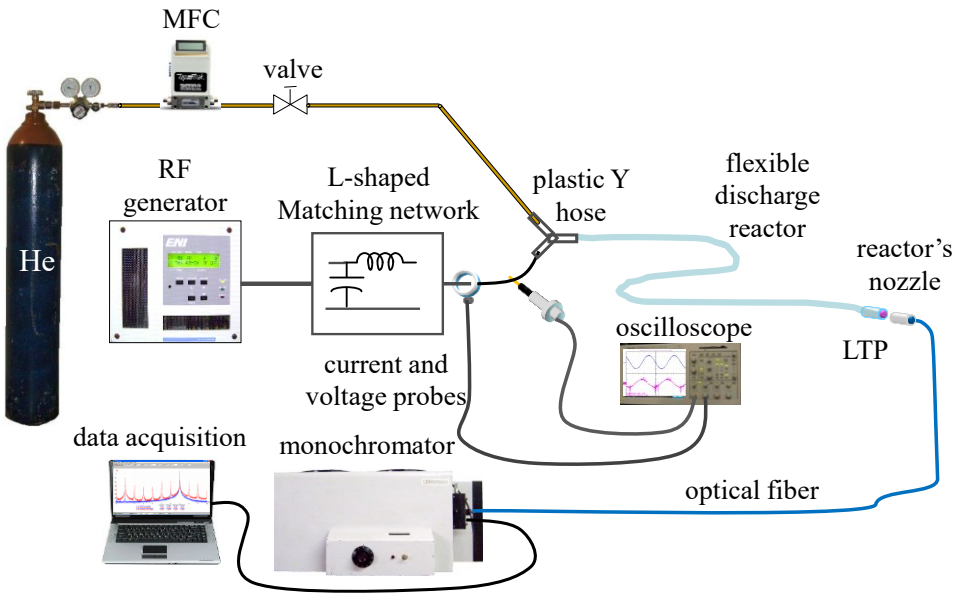

Fig. 1. Representation of the proposed LTP system, including the electrical instrumentation via high voltage and current probes associated with an oscilloscope and an optical array of a digital data acquisition associated with a monochromator coupled to an optical fiber located in front of the reactor's nozzle outlet.

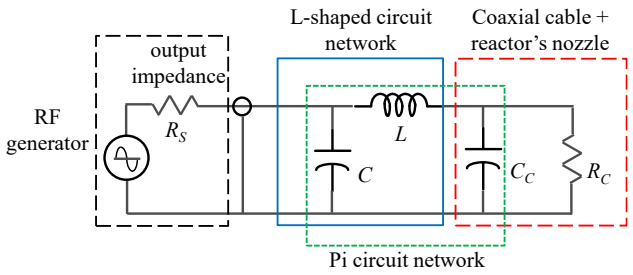

Fig. 2. Electric network representation for the electric load view from the RF source's output.

generator to the load without reflected power, providing a high electrical efficiency. The load circuit defined by the coaxial cable and the reactor's nozzle can be represented by the equivalent circuit network framed in the square with a dotted line in Fig. 2. It has been observed that the movement of the flexible reactor does not interfere with the LTP generation.

IV. LTP Characterization

A. Electric Characterization

The technique was implemented with a DPO2024B oscilloscope (Tektronix, Beaverton, U.S.) equipped with a P5100A (100X) high-voltage probe and a TCP2020 (10 mA/mV) current probe (Tektronix, Beaverton, U.S.) coupled with a special connector situated between the output of the matching network and the reactor's RF connector, as shown in the setup of Fig. 1.

The electrical characterization of the matching network coupled to the reactor is modified when the oscilloscope voltage probe is connected to the matching network output. This connection represents an addition of an equivalent load of 1 MΩ resistance associated in parallel with a capacitance of 14 pF. To compensate for this effect, the input capacitor was adjusted to match the nominal functioning behavior of the device, which, operating at 16 W, only reflects 1 W of power, providing a power transference of 94.11%, in comparison during the electric characterization when operating at 16 W, the reflected power was 4 W. The resulting electric working parameters of the LTP produced in helium supplied at 1.0 LPM for six different magnitudes of set-up generator RF power (P_{RF}) are included in Table I.

The voltage and current waveforms measured at the output of the matching network with an applied RF power of 12 W are presented in Fig. 3. The RF voltage waveform ($V_{RFp\text{-}p}$) exhibits a peak-to-peak value of approximately 340 V. In contrast, the RF current waveform ($I_{RFp\text{-}p}$) reaches a peak-to-peak value of 736 mA. The phase difference between these waveforms is consistent with the capacitive nature of the plasma charge at this frequency. It is relevant to highlight that, as detailed in Table I, an increasing trend is observed in both the peak-to-peak voltage and the peak-to-peak current as the applied RF power is selected from 10 W to 20 W, suggesting an increase in the energy density of the generated plasma. The reflected power (P_{REV}) remained low throughout the analyzed power range, indicating adequate power transfer efficiency due to the implementation of the designed matching network.

Fig. 4 shows a front view of the implemented device, operating under the conditions described above. The generated LTP, acting as a time-varying electromagnetic field source, produces an irradiance of 0.612 W/cm² when supplied with an RF power of 18 W. The resulting irradiance is below the maximum safe value for a non-ionizing radiation source, 4 W/cm² [44].

B. Optical Emission Characterization

Optical emission characterization of the generated plasma was achieved via a Czerny–Tuner monochromator model 305M (λ

TABLE I
ELECTRIC PARAMETERS

P_{RF} [W]	P_{FWR} [W]	P_{REV} [W]	$V_{RFp\text{-}p}$ [W]	$I_{RFp\text{-}p}$ [mA]
10	13	3	324	704
12	15	3	340	736
14	18	4	376	808
16	20	4	390	848
18	23	5	420	912
20	25	5	440	952

P_{RF} is the set-up generator RF power, P_{FWD} is the transmitted RF power, P_{REV} is the reflected RF power, $V_{RFp\text{-}p}$ is the peak-to-peak voltage and $I_{RFp\text{-}p}$ is the peak-to-peak current.

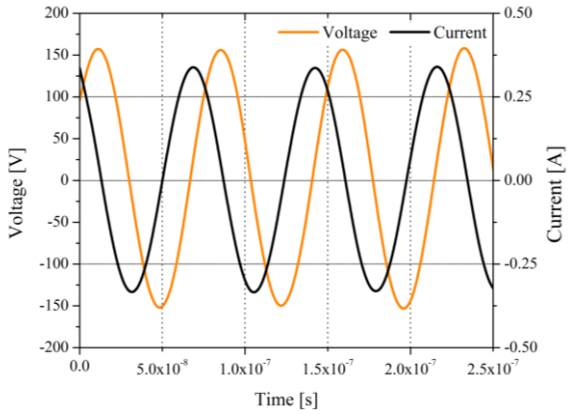

Fig. 3. Voltage and current waveforms measured at the matching box output with an RF applied power of 12 W.

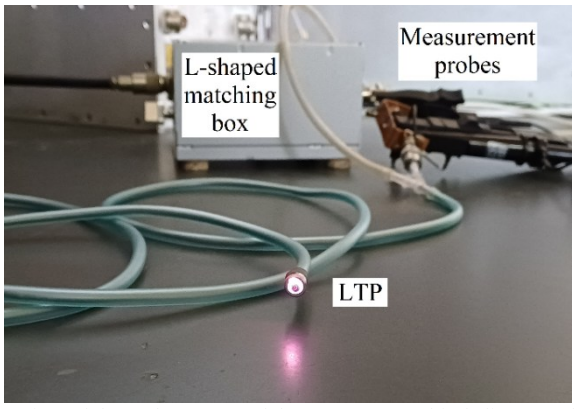

Fig. 4. View of the outlet reactor of the LTP generated in helium supplied at 1.0 LPM and applied RF power of 12 W.

Minuteman Laboratories Inc., Acton, U.S.) with a 0.5 m of focal length and a grating of 1200 grooves/mm coupled to a photomultiplier model R955 (Hamamatsu Photonics, Hamamatsu, Japan) and a data acquisition system, as it is represented in Fig. 1.

Optical fiber was put at a distance of two centimeters from the treatment probe's edge, pointing directly to the generated LTP in helium supplied at 1.0 LPM and an applied RF power of 12 W.

The spectrum presented in Fig. 5.(a) is distinctive of a plasma that is out of thermodynamic equilibrium with the occurrence of non–dominant N_2, OH and NOγ bands in the UV region. Therefore the first negative system of N_2^+ (B-X) was identified around 391.4 nm; the bands of the second positive system N_2 (C-B) spread between 330 to 380 nm; the OH (A-X) radical band commonly attributed to humid environmental air extends

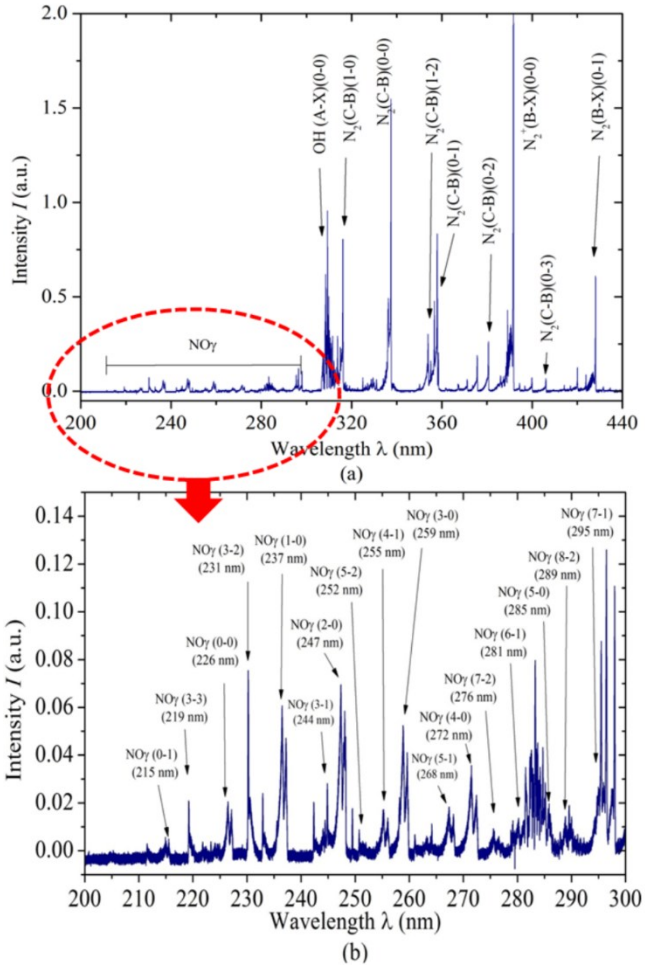

Fig 5. Optical emission spectrum of LTP generated with helium supplied at 1.0 LPM and an applied RF power of 12 W: (a) general view from 200 to 440 nm and (b) zoom view of UVC range determining the emission bands of NOγ.

TABLE II
MAIN REACTIONS IN LTP DISCHARGE

Reaction	Ref.	Equation
$H_2O + h\upsilon \rightarrow OH + H^+ + e^-$	[47]	(5)
$H_2O + e^- \rightarrow OH + H + e^-$	[48]	(6)
$OH + e^- \rightarrow OH(A) + e^-$	[48]	(7)
$He_2^+ + H_2O \rightarrow OH + HeH^+ + He$	[48]	(8)
$He_2^+ + N_2 \rightarrow 2He + N_2^+(B)$	[48]	(9)
$N_2(X) + e^- \rightarrow N_2(C) + e^-$	[49]	(10)
$N_2(X) + e^- \rightarrow N_2(A) + e^-$	[49]	(11)
$N_2(A) + e^- \rightarrow N_2(C) + e^-$	[49]	(12)
$N_2(X) + e^- \rightarrow N_2(B) + e^-$	[50]	(13)
$O_2 + e^- \rightarrow O + O(^1D) + e^-$	[49]	(14)
$N_2^* + O \rightarrow NO + N$	[47]	(15)

N_2^* represents any of the three above cited excited states of nitrogen molecule, whereas $N_2(X)$ represents its basal state.

between 307 to 309 nm; and the NOγ bands spanning from 215 to 295 nm are identified in the magnification image of Fig. 5.(b) [45], [46]. These excited molecules might be generated by chemical reactions from O_2, N_2 and H_2O present in the air; that were previously dissociated by: electronic collisions, excited molecules, UV radiation or metastable states of helium and subsequently excited and recombined through interactions with electrons or molecules (Table II) forming the spectra shown in Fig. 5. The production of RONS as a result of physicochemical

interactions of plasma with air molecules has been proved crucial for wound healing and skin diseases therapies, as RONS promote antisepsis and tissue regeneration. Therefore, LTP generators can be used as an alternative therapeutic instrument for wound healing. Moreover, as LTP generators become smaller, thinner and more flexible, they can reach regions inaccessible for rigid LTP generators.

C. UV Emission Characterization

The UV irradiation and temperature profile outcomes produced by the LTP established a measured separation between the reactor's nozzle and the sensor's surface detection by a one-axis mobile support arm. This last can hold the reactor while the separation distance is established by a screw structure situated at its opposite side. The LTP generates a broad UV radiation spectrum in which two regions could interact with biological molecules, predominantly the shortwave UV light that is considered an ionizing radiation. This is the reason why the produced UV radiation needs to be measured. UVx radiometer (Analytik Jena, Jena, Germany) associated with a UVX-25 shortwave detector 250-290 nm (UVC) and a UVX-31 midrange detector 280-340 nm (UVB) was employed.

The UV irradiance was characterized during normal functioning conditions of the LTP that was produced in helium flowing at 1.0 LPM at three different magnitudes of the applied RF electric power from 12 to 16 W in steps of 2 W. At the same time, each irradiation flux density was detected at ten different distances measured from the reactor's nozzle, starting at 1 mm and ending at 10 mm in steps of 1 mm. The measurements obtained from the UVB detector are depicted in Fig. 6, where a significant increase in irradiance flux density can be seen from distances less than 5 mm. The obtained outcomes for UVC generation are shown in Fig. 7. In both cases, the acquired values are lower than those produced by the natural solar irradiance flux density during a sunny day.

D. Temperature Profile Characterization

The temperature measurements were made using the previously mentioned one-axis mobile support arm and two different devices: a Northwest probe thermometer and a K-type thermocouple connected with a digital multimeter. The values obtained were averaged using three samples for each plotted point.

The temperature profile outcome produced by the LTP with working parameters determined by supplied helium at 1.0 LPM and an imposed RF electric power from 12 to 16 W in steps of 1 W is shown in Fig. 8. From this plot it can be seen that the generated temperature increases drastically at distances lesser than 3 mm, it is crucial to maintain a separation of minimum 4 mm between the reactor's nozzle and the surface to be exposed.

In addition, it is important to move the nozzle, making smooth, rounded movements over the surface under treatment. These guidelines are provided to avoid any biological risk produced by thermal damage. They have been successfully done for accelerate wound healing of: mice skin [14], acute neck radiodermatitis case [24], several wounds in lower extremities [26], diabetic foot [27], after removal of a neck tumor in a patient with HIV [29], and after biopsy on the gingiva and palate of a case series [51].

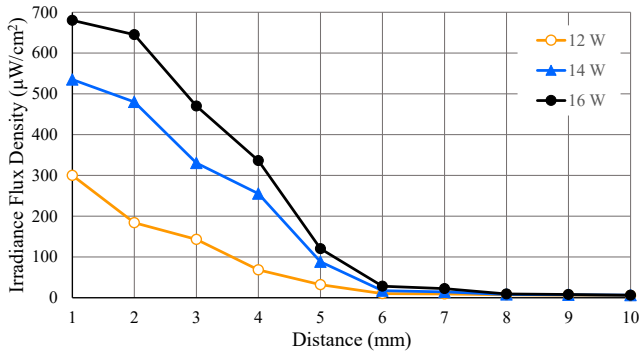

Fig. 6. UVB irradiance flux density longitudinal profile produced by the proposed LTP generated in helium flowing 1.0 LPM at three different supplied RF electric powers.

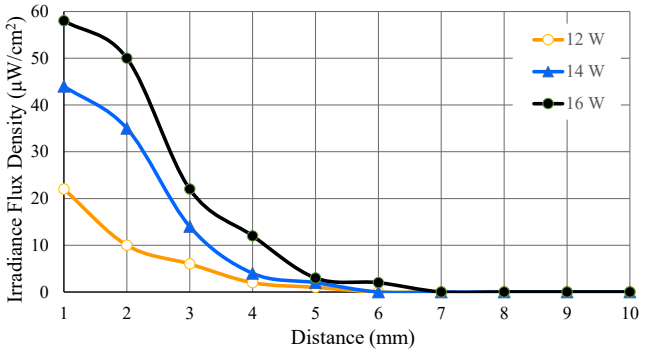

Fig. 7. UVC irradiance flux density longitudinal profile produced by the proposed LTP generated in helium flowing 1.0 LPM at three different supplied RF electric powers.

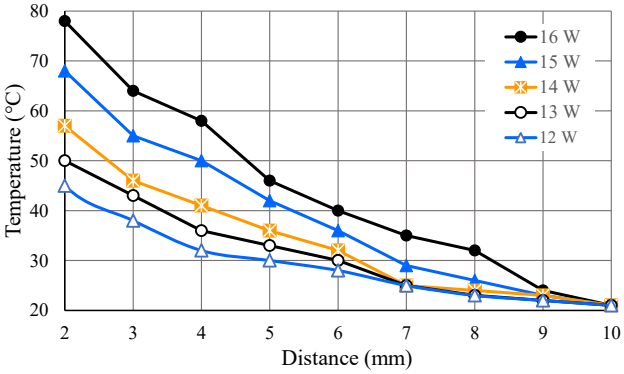

Fig. 8. Temperature longitudinal profile produced by the proposed LTP generated in helium flowing 1.0 LPM at five different supplied RF electric powers.

V. Bacteria Deactivation Trials

A. Method's Description for LTP Exposition on Agar Plate

Two different strains of microorganisms were utilized to determine the capability of the generated LTP to deactivate bacteria, a gram-negative bacterium, *Escherichia coli* and a gram-positive bacterium, *Enterococcus faecalis*. Both strains were prepared applying the same procedure described as follows: a single colony was cultured in Lysogeny broth for 24 h at 37 °C to obtain a microbiological concentration of around 10^8 bacteria/mL. The culture tubes were conditioned by double centrifugation at 5000 RPM for five minutes to remove the broth medium. Afterwards, the resulting sediment was re-suspended in 5 mL of buffer; from this, an aliquot of 100 μL was taken and diluted in 900 μL of distilled water, resulting in a concentration of around 10^7 bacteria/mL. A sample of 100

µL of this resulting media was diluted in 2 mL of liquid soft agar contained in a culture tube and maintained at 40 °C with a dry bath device. Later, each solution was spread throughout an agar plate previously prepared, resulting in an inoculation of around 10^6 bacteria per plate. Each inoculated agar plate was exposed to the LTP generated in helium supplied at a flow rate of 1.0 LPM and an RF electric power set up at one of three different magnitudes: 12, 14 and 16 W, the exposure times were established at 30, 60, 90 and 120 s, and the distance from the LTP reactor's nozzle to the agar surface was fixed at 4 mm. After the LTP treatment, the agar plates were incubated during 24 hr at 37 °C.

B. Deactivation of Escherichia Coli on Agar Plates

The results obtained for *E. coli* deactivation zones can be identified on the respective agar surface as transparent semicircles of different diameters, each situated at a quarter of the agar plate, as shown in Fig. 9. The bacterial deactivation of the last two cases were effective starting from 60 s of exposition time; these are portrayed in Fig. 9.b and Fig. 9.c. It has to be noted that there is no correlation between the amplitude of the applied RF electric power and the resulting deactivation zones.

This can be attributed to the distance between the reactor's nozzle and the treated surface, as well as the irregular surface of the agar. The agar plate can present micro-valleys and micro-hills, which can contain diverse concentrations of bacteria, making the inactivation process more difficult at higher concentrations. In this case, a better efficiency was obtained by applying an RF electric power of 14 W. The resulting inhibition zone diameters for the three applied RF powers were evaluated using ImageJ (v1.48s, National Institutes of Health, Bethesda, USA) and included in Table III.

C. Deactivation of Enterococcus Faecalis on Agar Plates

Fig. 10 shows the deactivation results of *Enterococcus faecalis* when exposed to LTP. It is important to note that this type of bacteria can cause severe infections, especially in healthcare settings, and is resistant to many commonly used antimicrobial agents. Additionally, *E. faecalis* has an effective DNA repair mechanism [52]. This characteristic makes it challenging to deactivate these bacteria. Nevertheless, the LTP generated at 16 W can deactivate *E. faecalis* after an exposure time of 60 s. The resulting inhibition zone diameters for the three different applied RF powers are included in Table IV.

D. Method's Description of LTP Exposition on Liquid

The same procedure describe in section *V* subsection *A. Method's description for LTP exposition on agar plate,* was developed to obtain a bacterial suspension at a concentration of 10^6 bacteria/mL. From this solution a series of six aliquot samples of 200 µL were deposited in wells of a microplate to be exposed to the LTP generated in helium supplied at a flow rate of 1.0 LPM and an applied RF electric power of 16 W, while the exposure times were established at 30, 60, 90, 120 and 180 s. Each sample was treated in triplicate. After the LTP treatment, two aliquots samples of 100 µL were taken from each well; one was directly spread on a Petri dish containing Lysogeny agar using a Drigalsky spatula and incubated during 24 hr at 37 °C. The other one was successively diluted until to obtain concentrations around 10^3 bacteria/mL, later spread it on agar plate and incubated during 24 hr at 37 °C. This procedure permit to realize the plate counting of each case.

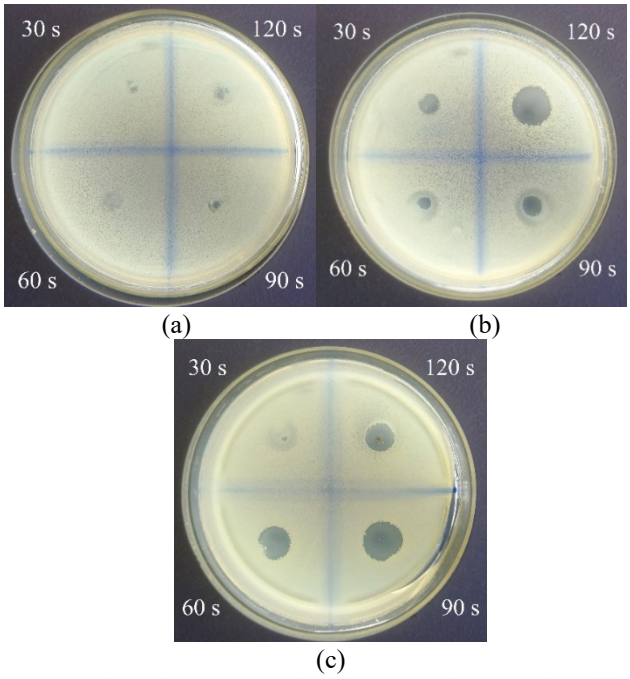

Fig. 9. Agar plates of *E. coli* CFU after being exposed to LTP at four different rate times 30, 60, 90 and 120 min, for each one of the three applied RF electric powers (a) 12 W, (b) 14 W and, (c) 16 W.

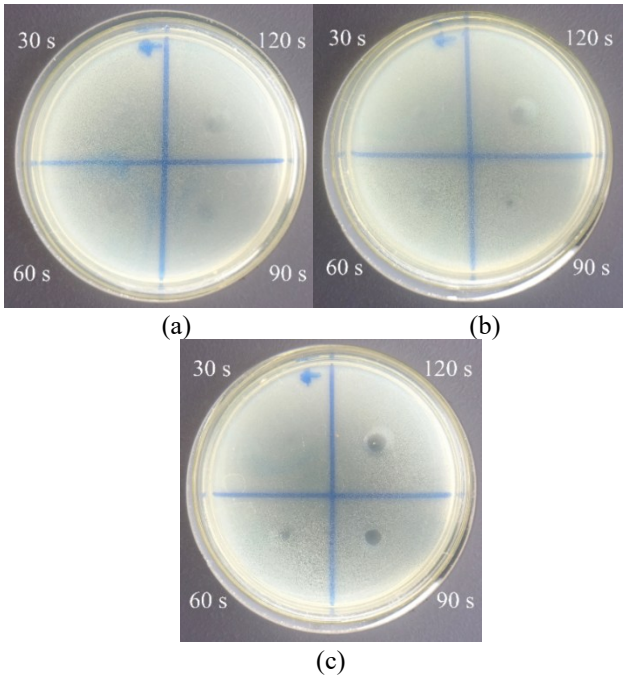

Fig. 10. Agar plates of *E. faecalis* CFU after being exposed to LTP at four different rate times 30, 60, 90 and 120 min, for each one of the three applied RF electric powers (a) 12 W, (b) 14 W and, (c) 16 W.

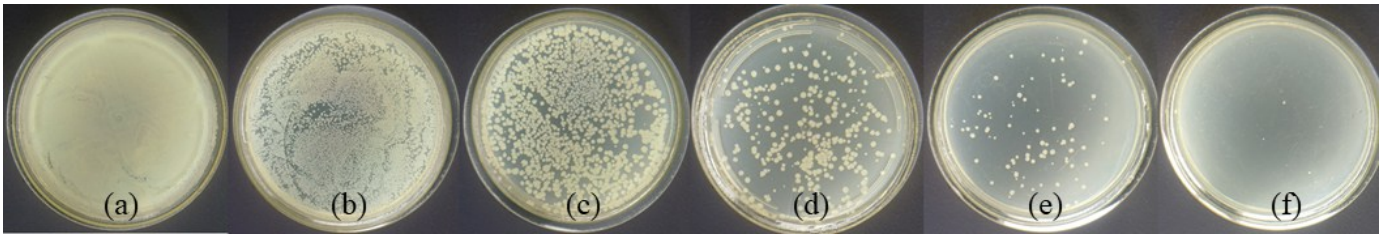

Fig. 11. CFU of *E. coli* after exposure to LTP generated at 16 W during: (a) control test ~3.6×10^6 CFU/mL, (b) 30 s, (c) 60 s, (d) 90 s, (e) 120 s and (f) 180 s.

TABLE III
INHIBITION ZONE DIAMETERS (*E. coli*)

	12 W		14 W		16 W	
Time [s]	M	σ	M	σ	M	σ
30	3.116	0.537	6.566	0.200	2.210	0.275
60	1.466	0.380	4.346	0.228	10.526	0.818
90	3.133	0.795	6.550	0.078	13.420	0.363
120	4.030	0.235	12.966	0.198	9.566	0.205

M is the main value and σ is the standard deviation in mm

TABLE IV
INHIBITION ZONE DIAMETERS (*E. faecalis*)

	12 W		14 W		16 W	
Time [s]	M	σ	M	σ	M	σ
30	0	0	0	0	0	0
60	0	0	0	0	2.780	0.180
90	0	0	1.716	0.321	5.260	0.310
120	0	0	0	0	6.033	0.162

M is the main value and σ is the standard deviation in mm

E. Deactivation of Escherichia Coli in Liquid

Fig. 11 shows the qualitative results of *E. coli* bacteria inactivation where Figure 11.a corresponds to the reference sample representing a concentration of ~3.6×10^6 CFU/mL, and Fig. 11.b to 11.f show the results after the different treatment time. It is notorious the bacteria elimination effect of the generated LTP that is reinforced with the drastic diminution of survability of *E. coli* shown in the graph of Fig. 12. The generated LTP attains a reduction of bacteria of 2.87-$\log_{10}$ at 120 s of treatment, reaching 4.43-$\log_{10}$ reduction at 180 s. While, the percentage of *E coli* inactivation in function of the exposure time to LTP is depicted in Fig. 13. The magnitude of *E. coli* inactivation achieved at 180 s was 99.996%.

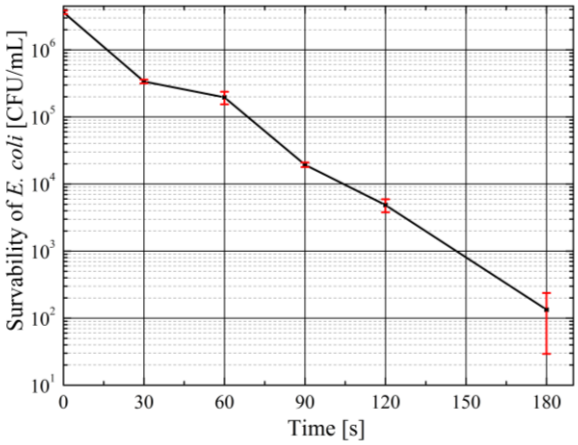

Fig. 12. Effect of LTP generated at 16 W on the viability of *E. coli* (Data reported are the mean of 3 experiments, and error bars determine the standard deviation).

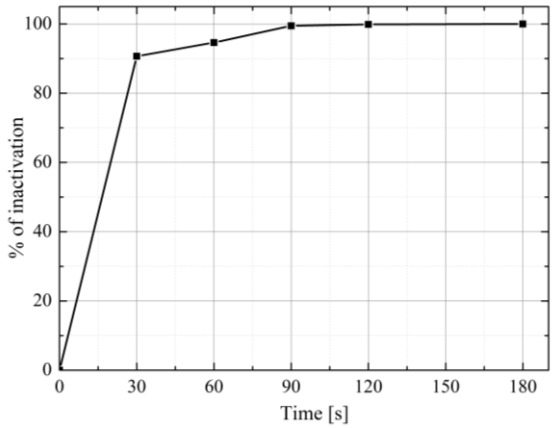

Fig. 13. Percentage *E. coli* inactivation of after exposition to LTP generated at 16 W.

VI. DISCUSSION

An innovative RF-driven flexible LTP source has been developed and characterized to explore its potential in various biomedical applications, as evidenced by the bacteria inactivation. This work's main contribution lies in the combination of a flexible design with a standard RF feed, enabling the generation of a non-thermal plasma rich in RONS. The following discussion focuses on comparing the characteristics and performance of the proposed flexible LTP device with the existing literature, highlighting its potential benefits and acknowledging its current limitations.

OES outcome revealed the presence of characteristic bands corresponding to various RONS, including fundamental species such as hydroxyl radical (OH), nitric oxide (NO), and excited nitrogen molecules (NOγ), in addition to the main reactions of LTP training the generation of atomic nitrogen (N) and oxygen (O) whose formation in the gas phase and solution is well known in low-temperature plasma systems [53]. These species are fundamental to the bioactivity of LTP, playing a crucial role in microbial inactivation and modulation of biological responses in tissues [54].

The bactericidal efficacy demonstrated through *in vitro* assays against *Escherichia coli* (gram-negative) and *Enterococcus faecalis* (gram-positive) can be attributed to the synergistic action of these RONS. It has been widely documented that plasma-generated RONS induce oxidative stress in bacterial cells, causing membrane lipid peroxidation, oxidation of essential proteins, and DNA damage, ultimately leading to loss of cell viability [55]. The lack of a direct

correlation between applied RF power and zones of inhibition in *E. coli* could suggest the influence of agar surface microtopography on the local distribution of RONS. This aspect warrants further investigation [56]. The increased resistance of *E. faecalis* to inactivation, observed in the need for higher RF power and exposure time, is consistent with the literature describing its efficient DNA repair mechanism [57].

The therapeutic potential of LTP is not limited to disinfection. At controlled concentrations, RONS also act as key mediators in mammalian tissue physiology. They have been shown to stimulate fibroblast proliferation [13], [58], accelerate wound healing [14], [59], promote re-epithelialization and angiogenesis [15], [60], and improve collagen availability [16], [61]. The ability of the proposed flexible device to generate RONS directly at the treatment site makes it a promising tool for applications in minimally invasive surgery, where precision and accessibility to complex areas are critical. The flexibility in the reactor's design represents a feature that could allow access to complex anatomical areas and navigation through narrow or curved ducts, which could be helpful in endoscopic or laparoscopic procedures.

Compared to other flexible plasma sources reported in the literature, such as microwave-based devices [40], dielectric barrier discharge [41], [42] or pulsed alternating current powered [43], an RF-based generator offers potential advantages in terms of stability and control in generating a specific RONS spectrum by optimizing gas flow and applied power [62]. Additionally, operation at a standard RF frequency of 13.56 MHz is common practice in biomedical applications, which could facilitate its integration into existing medical equipment [63].

Although the works of Liu *et al*. [40] and Nascimento *et al*. [43] also feature flexible designs, our RF-based implementation with a home-made matching network offers a unique combination that could translate into better control of plasma properties and ease of integration into flexible surgical tools. RF power enables precise control of the energy deposited into the gas, resulting in finer manipulation of plasma characteristics such as reactive species density and temperature, which is crucial for efficacy and safety in therapeutic applications [64]. While the home-made matching network optimizes the power transfer from the generator to the plasma, ensuring efficient and stable operation, which is critical for medical applications where treatment consistency is paramount [65]. The combination of a flexible design with the precise controllability inherent in RF plasma systems facilitates the potential integration of this technology into flexible endoscopic or laparoscopic tools, thereby expanding the reach of plasma-based therapies to anatomical regions previously inaccessible with rigid devices [66].

While our *in vitro* results are promising, it is critical to acknowledge the limitations of this initial study, particularly the lack of *in vivo* testing. However, it is essential to note that while the literature mentions the potential of LTP, specifically the NOγ band produced in our experiments, to promote wound closure [67]. Future research should focus on evaluating the device's biocompatibility, safety, and therapeutic efficacy of the device in animal models simulating relevant clinical scenarios. Furthermore, a direct comparative analysis with other commercially available LTP devices would be valuable in quantifying its advantages better and positioning it within the current technological landscape. Nevertheless, this work lays the groundwork for developing a versatile and potentially transformative therapeutic tool for minimally invasive surgery. This device could be applied in various scenarios, including decontaminating tissue surfaces after tumor resection, cauterizing small blood vessels, or stimulating healing in hard-to-reach areas. For example, it could be helpful in endoscopic procedures to treat gastric ulcers or injuries in the gastrointestinal tract. Furthermore, the possibility of using this flexible device in laparoscopic surgeries to treat internal tissues is envisioned.

This work presents the development and extensive characterization of an innovative RF-driven flexible LTP. Constructing a homemade matching network enabled efficient coupling to a commercial RF generator, optimizing plasma generation. Characterization of the plasma emission by means of OES revealed the presence of a distinct non-thermal equilibrium plasma rich in RONS, critical due to their bioactive properties. The device inactivated 99.996% of *E. coli* at a concentration of 3.6×10^6 CFU/mL in 180 s at 16 W, this inactivation corresponds a 4.43-log10 *E. coli* viability reduction, underscoring its potential as a tool for treatments focused on decontamination.

This initial characterization study suggests several promising therapeutic applications, including wound healing therapy following oesophageal, gastric, or cervical tissue biopsies and treating gastric ulcers and minor cervical injuries. The bacterial inactivation results also pave the way for its use in decontaminating irregular medical surfaces and treating superficial skin infections. The device's flexibility, combined with its ability to generate RONS with antimicrobial activity and the potential to stimulate tissue regeneration (as suggested by the presence of the NOγ band), positions it as an innovative alternative for minimally invasive procedures.

Despite the encouraging results obtained in this study, we acknowledge certain limitations, primarily the lack of *in vivo* testing that directly validates its efficacy and safety in complex biological models. Therefore, as future lines of research, we propose conducting studies in animal models to evaluate their biocompatibility and therapeutic potential in relevant clinical settings. Furthermore, optimizing the device's design to further improve its efficiency and exploring its application in other biomedical contexts, including laparoscopic surgeries for treating internal tissues, represent important avenues for the future development of this technology. Nevertheless, this work lays the groundwork for developing a versatile and potentially transformative therapeutic tool for minimally invasive surgery. This device could be applied in various scenarios, including decontaminating tissue surfaces after tumor resection, cauterizing small blood vessels, or stimulating healing in hard-to-reach areas. For example, it could be helpful in endoscopic procedures to treat gastric ulcers or injuries in the gastrointestinal tract. Furthermore, the possibility of using this flexible device in laparoscopic surgeries to treat internal tissues is envisioned.

VI. Conclusion

Microbial inactivation assays demonstrate that the developed non-thermal plasma (LTP) system effectively inactivates

gram-negative (*Escherichia coli*) and gram-positive (*Enterococcus faecalis*) bacteria on agar plates, and *E. coli* in liquid media. For *E. coli* on agar, effective inactivation was achieved with significant inhibition zones, with remarkable efficiency observed under optimized conditions. There was no direct linear correlation between applied RF power and zone diameter. For *E. faecalis*, a more resistant strain, inactivation was successful under appropriate exposure conditions, a significant result given its robust DNA repair mechanism. The efficacy of LTP in both solid and liquid environments, coupled with its low-temperature features, safe UV emission, and flexible design, highlights its promising potential for various microbial decontamination applications. It is certain that at this very moment, the breach to be able to realize experiences *in-vivo* represents a challenge to be solved, in order to consider the use of the proposed plasma source in laparoscopic surgeries, thus opening new avenues for innovative, minimally invasive antimicrobial treatments in internal cavities.

ACKNOWLEDGMENTS

The authors would like to thank the technical help provided from P. Angeles-Espinoza, I. Contreras-Villa, and M. T. Torres-Martínez, and the English assistance and proofreading received from M. Peña-Torres.

REFERENCES

[1] E. Stoffels, *et al*., "Plasma needle: a non-destructive atmospheric plasma source for fine surface treatment of (bio)materials," *Plasma Sources Sci. Technol*., vol. 11, no. 4, pp. 383–388, 2002, doi: 10.1088/0963-0252/11/4/304.

[2] K. Kelly-Wintenberg, *et al*., "Use of a one atmosphere uniform glow discharge plasma (OAUGDP) to kill a broad spectrum of microorganisms," *J. Vac. Sci. Technol*., vol. 17, no. 4, pp. 1539–1544, 1999, doi: 10.1116/1.581849.

[3] S. Lerouge, M. R. Wertheimer and L. Yahia, "Plasma Sterilization: A Review of Parameters, Mechanisms, and Limitations," *Plasmas Polym*., vol. 6, pp. 175–188, Sep. 2001, doi: 10.1023/A:1013196629791.

[4] M. Laroussi, "Sterilization of Contaminated Matter with an Atmospheric-Pressure Plasma," *IEEE Trans. Plasma Sci*., vol. 24, no. 3, pp. 1188–1191, Jun. 1996. doi: 10.1109/27.533129.

[5] M. Moisan, J. Barbeau, S. Moreau, J. Pelletier, M. Tabrizian and L. H. Yahia, "Low-temperature sterilization using gas plasmas: a review of the experiments and an analysis of the inactivation mechanisms," *Int. J. Pharma.*, vol. 226, no. 1–2, pp. 1-21, 2001, doi: 10.1016/S0378-5173(01)00752-9.

[6] J. C. Birmingham, "Mechanisms of Bacterial Spore Using Ambient Pressure Nonthermal Discharges," *IEEE Trans. Plasma Sci.,* vol. 32, no. 4, pp. 1526–1531, Aug. 2004, doi: 10.1109/TPS.2004.832609.

[7] T. Nosenko, T. Shimizu and G. E. Morfill, "Designing plasmas for chronic wound disinfection," *New J. Phys*, vol. 11, Nov. 2009, Art. no. 115013, doi: 10.1088/1367-2630/11/11/115013.

[8] J. Goree, B. Liu, D. Drake and E. Stoffels, "Killing of *S. mutans* Bacteria Using a Plasma Needle," *IEEE Trans. Plasma Sci*., vol. 34, no. 4, pp. 1317–1324, Aug. 2006. doi: 10.1109/TPS.2006.878431

[9] T. C. Montie, K. Kelly-Wintenberg and J. R. Roth, "An Overview of Research Using the One Atmosphere Uniform Glow Discharge Plasma (OAUGDP) for Sterilization of Surfaces and Materials," *IEEE Trans. Plasma Sci.,* vol. 28, no. 1, pp. 41–50, Feb. 2000, doi: 10.1109/27.842860

[10] E. Stoffels, I. E. Kieft and R. E. J. Sladek, "Superficial treatment of mammalian cells using plasma needle," *J. Phys. D: Appl. Phys*., vol. 36, pp. 2908–2913, 2003. [Online]. Available: stacks.iop.org/JPhysD/36/2908.

[11] D. Dobrynin, G. Fridman, G. Friedman and A. Fridman, "Physical and biological mechanisms of direct plasma interaction with living tissue," *New J. Phys*, vol. 11, Nov. 2009, Art. no. 115020, doi: 10.1088/1367-2630/11/11/115020.

[12] S. Coulombe, V. Léveillé, S. Yonson and R. L. Leask, "Miniature atmospheric pressure glow discharge torch (APGD-t) for local biomedical applications," *Pure Appl. Chem.*, vol. 78, no. 6, pp. 1147–1156, 2006, doi: 10.1351/pac200678061147.

[13] X. M. Shi, *et al*., "Low-temperature Plasma Promotes Fibroblast Proliferation in Wound Healing by ROS-activated NF-κB Signaling Pathway," *Curr Med Sci*., vol. 38, no. 1, pp. 107–114, Feb. 2018, doi: 10.1007/s11596-018-1853-x.

[14] E. García-Alcántara, *et al*., "Accelerated mice skin acute wound healing *in vivo* by combined treatment of argon and helium plasma needle," *Arch. Med. Res*., vol. 44, pp. 169–177, 2013, doi: 10.1016/j.arcmed.2013.02.001.

[15] M. Chatraie, G. Torkaman, M. Khani, H. Salehi and B. Shokri, "*In vivo* study of non-invasive effects of non-thermal plasma in pressure ulcer treatment," *Sci. Reports*, vol. 8, 2018, Art. no. 5621, doi: 10.1038/s41598-018-24049-z.

[16] S. K. Dubey, *et al*., "Cold atmospheric plasma therapy in wound healing," *Process Biochem.*, vol. 112, pp. 112–123, 2022, doi: 10.1016/j.procbio.2021.11.017.

[17] G. Fridman *et al*., "Floating Electrode Dielectric Barrier Discharge Plasma in Air Promoting Apoptotic Behavior in Melanoma Skin Cancer Cell Lines," *Plasma Chem. Plasma Proc.*, vol. 27, pp. 163–176, 2007, doi: 10.1007/s11090-007-9048-4.

[18] X. Yan, *et al*., "On the Mechanism of Plasma Inducing Cell Apoptosis," *IEEE Trans. Plasma Sci.,* vol. 38, no. 9, pp. 2451–2457, Sep. 2010, doi: 10.1109/TPS.2010.2056393.

[19] H. J. Lee, C. H. Shon, Y. S. Kim, S. Kim, G. C. Kim and M. G. Kong, "Degradation of adhesion molecules of G361 melanoma cells by a non-thermal atmospheric pressure microplasma," *New J. Phys*., vol. 11, 2009, Art. no. 115026, doi: 10.1088/1367-2630/11/11/115026.

[20] J. H. Serment Guerrero, K. Girón-Romero, R. López-Callejas and R. Peña-Eguiluz, "*In vitro* assessment of murine melanoma cells sensitivity to non-thermal atmospheric plasma," *J. Appl. Res. Technol*., vol. 17, pp. 180–185, 2019. [Online]. Available: https://jart.icat.unam.mx/index.php/jart/article/view/810/743

[21] I. Adamovich, *et al*., "The 2022 Plasma Roadmap: low temperature plasma science and technology," *J. Phys. D: Appl. Phys.,* vol. 55, pp. 22–25, 2022, Art. no. 373001, doi: 10.1088/1361-6463/ac5e1c.

[22] M. Betancourt-Ángeles *et al*., "Treatment in the healing of burns with a cold plasma source," *Int. J. Burns Trauma*, vol. 7, pp. 142–146, 2017. [Online]. Available: https://pmc.ncbi.nlm.nih.gov/articles/PMC5768930/

[23] C. Duchesne, S. Banzet, J.-J. Lataillade, A. Rousseau and N. Frescaline, "Cold atmospheric plasma modulates endothelial nitric oxide synthase signalling and enhances burn wound neovascularization," *J. Pathology*, vol. 249, no. 3, pp. 368–380, nov. 2019, doi: 10.1002/path.5323.

[24] R. Peña-Eguiluz, R. López-Callejas, B. González-Mendoza, A. Mercado-Cabrera, B. G. Rodríguez-Mendez and R. Valencia-Alvarado, "Acute Neck Radiodermatitis Treated by Nonthermal Plasma Therapy: Case Report," *IEEE Trans. Rad. Plasma Med. Sci*., vol. 6, no. 4, pp. 503–506, Apr. 2022, doi: 10.1109/TRPMS.2021.3070784.

[25] A. Chuangsuwanich, T. Assadamongkol and D. Boonyawan, "The Healing Effect of Low-Temperature Atmospheric-Pressure Plasma in Pressure Ulcer: A Randomized Controlled Trial," *Int. J. Lower Extremity Wounds*, vol. 15, no. 4, pp. 313–319, aug. 2016, doi:10.1177/1534734616665046.

[26] B. González-Mendoza, *et al*., "Healing of wounds in lower extremities employing a non-thermal plasma," *Clinical Plasma Med*., vol. 16, 2019, Art. no. e100094, doi: 10.1016/j.cpme.2020.100094.

[27] R. López-Callejas *et al*., "Alternative method for healing the diabetic foot by means of a plasma needle," *Clinical Plasma Med.*, vol. 9, pp. 19–23, 2018, doi: 10.1016/j.cpme.2018.01.001.

[28] R. He, *et al*., "The efficacy and safety of cold atmospheric plasma as a novel therapy for diabetic wound *in vitro* and *in vivo*," *Int. Wound J*., vol. 17, no. 3, pp. 851–863, Jun. 2020; doi: 10.1111/iwj.13341

[29] R. Peña-Eguiluz, *et al*., "Non-thermal plasma wound healing after removal of a neck tumor in a patient with HIV: A case report," *Otolaryngology Case Reports*, vol. 22, Jan. 2022, Art. no. 100391, doi: 10.1016/j.xocr.2021.100391.

[30] N. G. Ibáñez-Mancera, *et al*., "Wound Healing After Biopsy in the Mobile Oral Mucosa Using a Nonthermal Atmospheric Pressure Plasma," *IEEE Trans. Rad. Plasma Med. Sci*., vol. 6, no. 8, pp. 928–935, Nov. 2022, doi: 10.1109/TRPMS.2022.3161188

[31] N. G. Ibáñez-Mancera, *et al*., "Healing of Recurrent Aphthous Stomatitis by Non-Thermal Plasma: Pilot Study," *Biomedicines*, vol. 11, 2023, Art. no. 167, doi: 10.3390/biomedicines11010167.

[32] M. Vandamme, *et al*., "ROS implication in a new antitumor strategy based on non-thermal plasma," *Int. J. Cancer*, vol. 130, no. 9, pp. 2185–2194, May 2012, doi: 10.1002/ijc.26252.

[33] S. Kang, *et al*., "Nonthermal plasma induces head and neck cancer cell death: the potential involvement of mitogen-activated protein kinase-dependent mitochondrial reactive oxygen species," *Cell Death Dis.*, vol. 5, 2014, Art. no. e1056, doi:10.1038/cddis.2014.33.

[34] C. Song, P. Attri, S. K. Ku, I. Han, A. Bogaerts and E H. Choi, "Cocktail of reactive species generated by cold atmospheric plasma: oral administration induces non-small cell lung cancer cell death," *J. Phys. D: Appl. Phys*., vol. 54, no. 18, 2021, Art. no. 185202, doi: 10.1088/1361-6463/abdff2.

[35] H. Tanaka, S. Bekeschus, D. Yan, M. Hori, M. Keidar and M. Laroussi, "Plasma-Treated Solutions (PTS) in Cancer Therapy", *Cancers*, vol. 13, no. 7, Apr. 2021, Art. no. 1737, doi: 10.3390/cancers13071737.

[36] G. Neretti, *et al*., "Characterization of a plasma source for biomedical applications by electrical, optical, and chemical measurements," *Plasma Proc. Polym*., vol. 15, no. 11, Nov. 2018, Art. no. 1800105, doi: 10.1002/ppap.201800105.

[37] T. von Woedtke, M Laroussi and M Gherardi, "Foundations of plasmas for medical applications," *Plasma Sources Sci. Technol*., vol. 31, no. 5, 2022, Art. no. 054002, doi: 10.1088/1361-6595/ac604f.

[38] K.-D. Weltmann and T. von Woedtke, "Basic requirements for plasmas sources in medicine," *Eur. Phys. J.: Appl. Phys.,* vol. 55, Jul. 2011, Art. no. 13807, doi: 10.1051/epjap/2011100452.

[39] R. Peña-Eguiluz, *et al*., "Development and Characterization of a Non-Thermal Plasma Source for Therapeutic Treatments", *IEEE Trans. Biomed. Eng.,* vol. 68, no. 5, pp. 1467–1476, May 2021, doi: 10.1109/TBME.2020.3041195.

[40] T. Liu, *et al*., "Design of a Flexible Microwave-Induced Room-Temperature Atmospheric-Pressure Microwave Source," *IEEE Trans. Plasma Sci.,* vol. 52, no. 3, pp. 652–656, Mar. 2024, doi: 10.1109/TPS.2024.3376526.

[41] C. Corbella and S. Portal, "Flexible plasma multi-jet source operated in radial discharge configuration," *Rev. Sci. Instrum*., vol. 92, no. 12, Dec. 2021, Art. no. 123502, doi: 10.1063/5.0068219.

[42] O. Bastin, *et al*., "Optical and Electrical Characteristics of an Endoscopic DBD Plasma Jet," *Plasma Med*., vol. 10, no. 2, pp 71–90, 2020, doi: 10.1615/PlasmaMed.2020034526.

[43] F. do Nascimento, *et al*., "A Low Cost, Flexible Atmospheric Pressure Plasma Jet Device with Good Antimicrobial Efficiency," *IEEE Trans. Rad. Plasma Med. Sci.,* vol. 8, no. 3, pp. 307–322, Mar. 2024, doi: 10.1109/TRPMS.2023.3342709.

[44] International Commission on Non-Ionizing Radiation Protection, "ICNIRP statement on diagnostic devices using non-ionizing radiation: Existing regulations and potential health risks," *Health Phys*., vol. 112, no. 3, pp. 305–321, Jan. 2017, doi: 10.1097/HP.0000000000000654.

[45] R. W. B. Pearse and A. G. Gaydon, *The identification of molecular spectra*, London, England: Chapman & Hall LTD., 1941, pp. 1–276. [Online]. Available: https://archive.org/details/in.ernet.dli.2015.212925.

[46] A. G. Gaydon, "The band spectrum of NO: The gamma and epsilon systems," *Proc. Phys. Society*, vol. 56, no. 2, pp. 95–-103, 1944, doi: 10.1088/0959-5309/56/2/305.

[47] S. Reuter, T. von Woedtke and K.-D. Weltmann, "The kINPen–a review on physics and chemistry of the atmospheric pressure plasma jet and its applications," *J. Phys. D: Appl. Phys*., vol. 51, no. 23, 2018, Art. no. 233001, doi: 10.1088/1361-6463/aab3ad.

[48] V. V Kovačević, B. P. Dojčinović, M. Jović, G. M. Roglić, B. M. Obradović and M. M. Kuraica, "Measurement of reactive species generated by dielectric barrier discharge in direct contact with water in different atmospheres," *J. Phys. D: Appl. Phys*., vol. 50, 2017, Art. no. 155205, doi: 10.1088/1361-6463/aa5fde.

[49] S. Wang, D. Yang, F. Liu, W. Wang and Z. Fang, "Spectroscopic study of bipolar nanosecond pulse gas-liquid discharge in atmospheric argon," *Plasma Sci. Technol*., vol. 20, no. 7, 2018, Art. no. 075404, doi: 10.1088/2058-6272/aabac8.

[50] I. A. Kossyi, A. Y. Kostinsky, A. A. Matveyev and V. P. Silakov, "Kinetic scheme of the non-equilibrium discharge in nitrogen-oxygen mixtures," *Plasma Sources Sci. Technol*., vol. 1, no. 3, pp. 207–220, 1992, doi: 10.1088/0963-0252/1/3/011.

[51] N. G. Ibáñez-Mancera, *et al*., "Cold Atmospheric Plasma Benefits after a Biopsy on the Gingiva and Palate: A Case Series," *Plasma Med*, vol. 12, no. 4, pp. 1–9, Dec. 2022, doi: 10.1615/PlasmaMed.2022045686

[52] K. P. Ha, R. S. Clarke, G. Kim, J. L. Brittan, J. E. Rowley, et al., "Staphylococcal DNA repair is required for infection", *mBio*, vol. 11, no. 6, 2020, doi: 10.1128/mbio.02288-20.

[53] L. Pinard, and C. Batiot-Dupeyrat, "Non-thermal plasma for catalyst regeneration: A review," *Catal. Today*, vol. 426, Jan. 2024, Art. no. 114372, doi: 10.1016/j.cattod.2023.114372.

[54] Y. Xu, and A. Bassi, "Non-thermal plasma decontamination of microbes: a state of the art," *Biotechnol. Prog*., vol. 41, no. 2, Mar.-Apr. 2025, Art. no. e3511, doi: 10.1002/btpr.3511.

[55] S. G. Scaltriti, A. Cristofolini, and G. Neretti, "Design and Characterization of an Atmospheric Pressure Dielectric Barrier Discharge Reactor for Potential Air Disinfection Applications," *IEEE Access*, vol. 13, Mar. 2025, Art. no. e45037, doi: 10.1109/ACCESS.2025.3548933.

[56] A. Helmke, I. Curril, J. Mrotzek, J. Schulz, and W. Viöl. "Non-thermal plasma for decontamination of bacteria trapped in particulate matter filters: plasma source characteristics and antibacterial potential," *J. Phys. D: Appl. Phys.,* vol. 57, no. 26, Apr. 2024, Art no. 265202, doi: 10.1088/1361-6463/ad35d3.

[57] A. H. Marx, H. Oltmanns, J. Meißner, J. Verspohl, T. Fuchsluger, and C. Busse. "Argon cold atmospheric plasma eradicates pathogens *in vitro* that are commonly associated

with canine bacterial keratitis," *Front. Vet. Sci.,* vol, 10, 2023, Art. no. 1320145, doi: 10.3389/fvets.2023.1320145.
[58] J. Stoof, et al., "Non-thermal plasma as promising anti-cancer therapy against bladder cancer by inducing DNA damage and cell cycle arrest," *Sci. Rep.,* vol. 1, Jan. 2025, Art. no. 2334, doi: 10.1038/s41598-025-85568-0.
[59] R. Shoorgashti, R. Nikmaram, Y. Azimi, A. Rouientan, H. Ebrahimi, and S. Lesan, "Effectiveness of cold plasma application in oral wound healing process: A scoping review," *Oral Dis*., vol. 30, no. 8, pp. 5062–5081, Nov. 2024, doi: 10.1111/odi.15119.
[60] E. Biscop, *et al*., "Dose-dependent induction of epithelial-mesenchymal transition in 3D melanoma models by non-thermal plasma treatment," *Mol. Oncol.*, early access, doi: 10.1002/1878-0261.70055.
[61] T. Sharfuddin, D. Jacho, D. Mitchey, E. Yildirim-Ayan, and H. Ayan, "A Study on the Effect of Non-thermal Plasma on Macrophage Phenotype Modulation," *Plasma Chem. Plasma Proc.,* vol. 44, pp. 455–470, Jan. 2024, doi: 10.1007/s11090-023-10414-y.
[62] T. Dufour, "From Basics to Frontiers: A Comprehensive Review of Plasma-Modified and Plasma-Synthesized Polymer Films," *Polymers*, vol. 15, no. 17, 2023, Art. no. 3607, doi: 10.3390/polym15173607.
[63] M. A. Ansari, *et al*., "Characterization of Plasma Discharge in a Multi Dipole Line Cusp Magnetic Field Created by an RF Source Coupled by a Spiral Antenna," *IEEE Trans. Plasma Sci*., vol. 51, no. 3, pp. 625–631, Mar. 2023, doi: 10.1109/TPS.2023.3251384.
[64] J. E. Thomas and K. Stapelmann, "Plasma Control: A Review of Developments and Applications of Plasma Medicine Control Mechanisms," *Plasma*, vol. 7, no. 2, pp. 386–426, May 2024, doi: 10.3390/plasma7020022.
[65] A. Zerehpoush, Z. R. Mobaraki, H. Afarideh and H. Rahimpour, "An Automatic Impedance Matching Network Based on Neural Network Technique for Inductive RF Plasma Source," *IEEE Trans. Instrum. Meas.*, vol. 74, Mar. 2025, Art. no. 2513009, doi: 10.1109/TIM.2025.3544285.
[66] J. Apelqvist, *et al*., "Cold plasma: an emerging technology for clinical use in wound healing," *J. Wound Manage.*, vol. 25, no. 3, pp. S1–S84, 2024; doi: 10.35279/jowm2024.25.03.sup01.
[67] H. R. Lee, *et al*., "Liquid plasma as a treatment for cutaneous wound healing through regulation of redox metabolism," *Cell Death Dis*., vol 14, Feb. 2023, Art. no. 119, doi: 10.1038/s41419-023-05610-9.

Rosendo Peña-Eguiluz (Member, IEEE) received his B.Sc., and M.Sc. in Electronic Engineering from Instituto Tecnológico de Toluca, and an Eng.D. in Electrical Engineering from Institut National Polytechnique de Toulouse, France. He currently serves as a Full-Time Researcher at the Instituto Nacional de Investigaciones Nucleares, Mexico. His primary research focuses on electric power converters, plasma generators, RF amplifiers, plasma medicine, plasma applications, and applied digital control. He is the author of several publications in indexed journals and international events.

Antonio Mercado-Cabrera received his M.Sc., and Ph.D. in Plasma Physics and Engineering, with specialization in radiative coefficient calculations, chemical kinetics, and modeling of thermal plasmas, from Paul Sabatier University, France. Currently, Antonio is a Full-Time Researcher at the Instituto Nacional de Investigaciones, Mexico. His currently research interests include chemical kinetics, computational fluid dynamics for air pollution control, and new technologies for wastewater treatment. He is the author of several publications in indexed journals and international events.

Alma N. Hernández-Arias received her B.Sc. in Chemical Engineering, and a Ph.D in Electronic Engineering from the Instituto Tecnológico de Toluca, Mexico. She currently serves as Teacher of subject at the Universidad Tecnológica del Valle de Toluca, Mexico. Her current research interests include new technologies for water remediation, water microorganism deactivation by plasma, and advanced oxidation processes. She is the author of several publications in indexed journals and international events.

Benjamín G. Rodríguez-Méndez received his Ph.D in Electronic Engineering from the Instituto Tecnológico de Toluca, Mexico. He is currently a Full-Time Researcher at the Instituto Nacional de Investigaciones Nucleares, Mexico. He actually is focusing on power electronics for the electrical discharges generation and plasma applications. His current research interests include modeling, and electronic instrumentation in plasma sciences. He is the author of several publications in indexed journals and international events.

Régulo López-Callejas received his Ph.D. in Electronic Engineering from the Instituto Tecnológico de Toluca, Mexico. He is a Full-Time Researcher of Plasma Physics Instrumentation at the Instituto Nacional de Investigaciones Nucleares, Mexico. His current research interests include plasma applications, and electronic instrumentation. He is the author of several publications in indexed journals.

Raúl Valencia-Alvarado received his Ph.D. in Nuclear Science from the Universidad Autónoma del Estado de México, Mexico. He is a Full-Time Researcher at the Instituto Nacional de Investigaciones Nucleares, Mexico. His current research interests include the plasma processing of materials. He is the author of several publications in indexed journals.

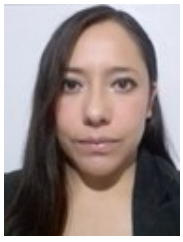

Bethsabet Jaramillo-Sierra received her B.Sc. in Chemical Engineering and a Ph.D. in Electronic Engineering from the Instituto Tecnológico de Toluca, Mexico. She actually serves as full-time profesor at the Tecnológico de Estudios Superiores de Tianguistenco, Mexico. Her current research interests include new technologies for water remediation, advanced oxidation processes, pollution control, and chemical kinetics. She is the author of several publications in indexed journals and international events.